Los Alamos National Laboratory is operated by the University of California for the United States Department of Energy under contract W-7405-ENG-36

LA-UR--92-2155

DE92 018897

TITLE Reactant Gas Flow Fields in Advanced PEM (Proton Exchange Membrane) Fuel Cell Designs

AUTHOR(S) Michael C. Kimble, and Nicholas E. Vanderborgh

SUBMITTED TO 27th Intersociety Energy Conversion Engineering Conference
Town and Country Hotel
San Diego, CA
August 3-7, 1992

## DISCLAIMER







Los Alamos Los Alamos National Laboratory
Los Alamos, New Mexico 87545

# Reactant Gas Flow Fields in Advanced PEM Fuel Cell Designs

Michael C. Kimble and Nicholas E. Vanderborgh
Advanced Engineering Technology/MEE-13
Los Alamos National Laboratory
Los Alamos, NM 87545

## ABSTRACT

A mathematical model of the two-phase flow in a fuel cell gas channel is developed and used to predict the mass, momentum, and thermal distributions of a multi-component gas and liquid water mixture on the cathode side. Regions where flooding may occur are demonstrated by using the model evaluated with various operating conditions typical of fuel cell operations. Conditions where dry, saturated, and two-phase flows are introduced into the channel are demonstrated and the results compared. These results show the distribution of water and heat in the channel which may be used to design better flow channels.

## INTRODUCTION

Previous advances on the proton exchange membrane (PEM) fuel cell have resulted in designs now competitive with other electrochemical power sources, both from an economic and a power producing basis. Research advances in ultra-thin membrane separators, thin film electrodes, and low platinum loadings have led to high power densities within potentially low cost devices. Other stack components, for instance, the anode and cathode gas flow fields are less advanced than the membrane and electrode assemblies. Each of these flow fields is positioned between an electrode and the bipolar plate as shown in Fig. 1. Flow fields must permit gaseous and liquid mass flow while maintaining adequate electronic conductivity. Large area flow field designs demonstrate scaling problems in thermal and mass management not seen in small, single cells. A typical problem is liquid water accumulation which inhibits gas transport resulting in decreased fuel cell performance. One of the important tasks that needs to be addressed is the optimal flow geometry of the reactant gas flow fields. In order to obtain high fuel cell performance, it is necessary to maintain sufficiently high reactant concentration while preventing either excess water hydration or dehydration. Also of importance is the distribution of heat which has a strong impact on fuel cell performance by affecting, for example, water and species transport as well as reflecting the electrochemical reactions in the electrodes. Required control of this thermal management is necessary to maintain stable, high performance as discussed by Vanderborgh *et al.* [1].

A mathematical model of the gas and liquid flow in the gas channel can give a better understanding of this complex phenomena which may lead to better water and thermal management in the fuel cell. The model developed for this work considers the mass distribution of the gases ($O_2$, $N_2$, and $H_2O$), the mass distribution of liquid $H_2O$, the momentum distribution of the gas phase and of the liquid phase, and the thermal distribution of the combined gas and liquid phases. Also, since the gas and liquid phase volumes change throughout the gas channel, these volume changes are accounted for in the model. By considering the transport of each phase separately, more realism is included in the model with less reliance on empirical correlations. The development of the phenomenological equations will be described next.

## MODEL DEVELOPMENT

A conceptualization of the two-phase flow channel is shown in Fig. 2. Note that each phase is assumed continuous and separate in order that continuum conservation equations may be applied to each phase. As the gas flows down the channel, $O_2$ is consumed by the electrochemical reaction while some of the $H_2O$ produced by the reaction enters the gas channel. As more and more water enters the channel, the cross-sectional area for flow of the gas and liquid phases changes, which causes the velocities of each phase to change. These varying velocities throughout the channel will influence the mass and thermal distributions in the flow channel. The heat brought into the channel with the convective flow, consumption/production of species into the fuel cell, condensation/evaporation, and heat loss through the channel walls affects the temperature of the gas-liquid mixture. Hence, the varying temperature, cross-sectional area (volume), consumption of $O_2$, and production of $H_2O$ changes the density of the mixture and must be accounted for in the model.

The variables of interest in this work are the concentrations, $C_i$, (mol/cm$^3$) of oxygen, nitrogen, and water in the gas phase, the number of moles, $n_w$, of liquid water, the velocity (cm/s) of the gas phase, $v^g$, and liquid phase, $v^l$, the cross-sectional areas (cm$^2$) for flow of the gas phase, $A^g$, and liquid phase, $A^l$, in the channel, and the temperature (K) of the two-phase mixture, $T$. The equations necessary to describe the gas and liquid flow are the equation of continuity for each gas species $i$ and liquid water, an equation of motion for each phase, a conservation of area (volume) equation, a liquid water density correlation, and a conservation of energy

expression. In order to gain more accuracy with the model and to use as few correlations or empiricisms as possible, the conservation equations are applied to each phase. Quasi one-dimensional conservation equations are formulated since the cross-sectional area for flow is not constant [2]. A mass balance taken about a volume element where the velocity, density, and cross-sectional area for flow may vary results in the following steady-state equation:

$$0 = -\frac{d}{dx}(C_i v^g A^g) + R_i^g W \tag{1}$$

where $R_i^g$ is the production rate (mol/cm$^2$-s) for a gaseous species $i$ and $W$ is the width of the channel. A similar expression can be used for the liquid water:

$$0 = -\frac{d}{dx}(C^l_{H_2O} v^l A^l) + R^l_{H_2O} W \tag{2}$$

Since water is the only species in the liquid phase, the density of water, based on tabulated values [3], can be used to express the liquid phase cross-sectional area for liquid flow as given by:

$$A^l = \frac{n_{H_2O} M_{H_2O}}{\rho(T)\,\Delta x} \tag{3}$$

where $\Delta x$ is the step size in the spatial discretization of the flow channel used in solving the system of equations and $M_i$ is the molecular weight of species $i$. The total cross-sectional area, $A^T$, of the gas channel is constant which allows the gas phase area for flow to be readily obtained:

$$A^g = A^T - A^l \tag{4}$$

The reaction rate expressions in Eqs. (1) and (2) correspond to the production or consumption of a species in the fuel cell which, for this work, are given as a function of the local current density and the stoichiometry of the electrochemical reactions. Hence, for a given current density, $j$ (A/cm$^2$), the oxygen reaction rate is:

$$R^g_{O_2} = -\frac{j}{4F} \tag{5}$$

The reaction rate for $N_2$ is set to zero which assumes that no cross-over of nitrogen occurs from the cathode to the anode. This condition could, of course, be changed to account for the cross-over effect, but is not considered for this work. Based on the overall reaction in the PEM fuel cell, twice as much water is produced as oxygen is consumed. Of the water produced, a certain fraction, $f_c$, leaves through the cathode with the remainder leaving through the anode. For simplicity, this fraction is set to a value to perform the calculations. A more rigorous approach could be used to include the gas and liquid transport across the fuel cell (electrodes and separator). This would require accurate knowledge of the transport parameters such as the water diffusion coefficient. However, as discussed by Vanderborgh *et al.* [4], the interfacial transport processes across the system may not be represented by equilibrium conditions which are typically used to measure diffusivities and electro-osmotic drag coefficients. Hence, the rate of water production in the cathode is

$$R_{H_2O} = \frac{2j}{4F} f_c \tag{6}$$

The model treats any liquid water entering the flow channel as going first to the vapor state until the saturation point is reached. Once the gas is saturated, any water entering the channel will then contribute to the liquid state of the channel.

The equation of motion is written for each phase to give the gaseous and liquid phase velocities. Applied to the gas phase, the appropriate conservation expression simplifies to:

$$0 = -\frac{d}{dx}(\rho^g v^g v^g A^g) + \psi \tag{7}$$

where the gas phase density is

$$\rho^g = C_{O_2} M_{O_2} + C_{N_2} M_{N_2} + C^g_{H_2O} M_{H_2O} \tag{8}$$

and where $\psi$ is an interfacial acceleration term formulated by consideration of the inertial forces in a volume element between the two phases based on a changing cross-sectional flow area.

$$\psi = (\rho^l v^l v^l - \rho^g v^g v^g)\frac{dA}{dx} \tag{9}$$

Equation (9) allows part of the momentum of one phase to be transferred to the other phase based solely on inertial effects. Note that in Eq. (7) the only significant term in the equation of motion is the inertial effect. Based on the Re number, inertial effects are more dominant than the viscous effects for this type of flow system. Assuming a constant pressure over the short length of the flow channel, pressure effects are also neglected. This assumption could be changed by incorporating an accurate equation of state for the two-phase, multi-component mixture. The liquid phase velocity is given by a similar expression to Eq. (7):

$$0 = -\frac{d}{dx}(\rho^l v^l v^l A^l) - \psi \tag{10}$$

An average temperature of the gas and liquid phases is calculated by accounting for the heat flux entering the channel from the walls and from the heat flux due to the production/consumption of species into the channel due to reaction in the fuel cell and flow effects. Thus, the equation of energy becomes:

$$\frac{d}{dx}\left(\left[C^g_{O_2} c_{p,O_2} + C^g_{N_2} c_{p,N_2} + C^g_{H_2O} c^g_{p,H_2O}\right] v^g T + (C^l_{H_2O} c^l_{p,H_2O} v^l T)\right) =$$

$$\frac{4k(T - T_{wall})}{D^2} - \frac{4k(T - T_{wall})}{W^2} + \frac{H^g_{O_2} R^g_{O_2}}{D} + \frac{H^g_{H_2O} R^g_{H_2O}}{D} + \frac{H^l_{H_2O} R^l_{H_2O}}{D} + \frac{\Delta H_{vap} R^g_{H_2O}}{D} \tag{11}$$

where $c_{p,i}$ is the heat capacity of species $i$, $k$ is an area averaged

thermal conductivity for the mixture, and $H_i$ is the enthalpy for species $i$. Note that the term on the left hand side of Eq. (11) represents the heat brought into the channel due to flow, the first and second terms on the right hand side correspond to heat loss/gain through the channel walls where $T_{wall}$ is the temperature of the wall, and the remainder of the terms in Eq. (11) represent the heat brought into or out of the channel due to the production or consumption of $H_2O$ and $O_2$, respectively.

## RESULTS AND DISCUSSION

In order to simulate the flow through the serpentine flow path as shown in Fig. 1, a continuous straight channel was assumed for the simulation so that quasi one-dimensional equations could be used. Equations (1) - (11) were solved numerically by second-order accurate finite difference approximations. A set of base case parameters, shown in Table 1, were used corresponding to a single cell with an active area of 46.45 $cm^2$ (1/20 $ft^2$). Three different inlet conditions (two-phase flow, relative humidity = 0 and 100%) were selected reflecting the most probable modes of operation in the channel and the resulting mass, momentum, and thermal distributions compared from the model results. These type of flow conditions may occur on the cathode side of fuel cell stacks either at inlet or end-plate assemblies or at internal cell assemblies in the stack.

In Fig. 3, the number of oxygen moles as a function of the dimensionless channel length are shown for the different inlet conditions. Since the gas phase volume may change down the fuel cell length, the number of moles of oxygen is given rather than the oxygen concentration. Note that for the two-phase inlet flow case, the volumetric flow rate for the liquid phase was set to the same volumetric flow rate of the gas phase where the gas flow rate corresponds to the conditions shown in Table 1. As shown in Fig. 3, the number of oxygen moles does not follow a linear relationship with the distance down the channel due to the changing momentum effects in the channel. This effect would be enhanced with additional manifolds of the cathode flow in the stack resulting in lower than expected oxygen concentrations in downstream regions of the fuel cell stack. Consequently, the driving force for oxygen diffusion into the electrode layers of the cell is decreased. This lowering of the oxygen concentration would be expected to lower the electrochemical activity of the fuel cell as governed by Butler-Volmer electrochemical kinetics. Changes in the local current density would then influence additional transport processes, however, this effect is beyond the scope of the present work. Of particular importance in Fig. 3 is the oxygen mole distribution for a two-phase inlet flow. Since the liquid phase occupies a significant fraction of the overall channel volume, increasing the amount of liquid water in the channel (due to the electrochemical reaction) decreases the cross-sectional area for flow of the gas phase. This creates a converging duct for the gas phase resulting in an increasing gas phase velocity. In order to conserve the mass and momentum of the gas phase as governed by Eqs. (1) and (7), the oxygen density simultaneously decreases. Hence, the liquid flow results in a much lower number of oxygen moles in the channel resulting in lower electrochemical activity as described above.

The temperature distribution in the flow channel is shown in Fig. 4 for various inlet conditions. For the dry inlet flow at 298 K, the gas temperature increases quickly within about 25% of the channel to a uniform temperature set by the channel wall temperature and the temperature of the neighboring electrode layer. The liquid water entering the channel from the electrochemical reaction is vaporized until the gas is saturated, as shown in Fig. 5, at approximately 40% into the channel. Depending on the inlet temperature, this vaporization process can cause a negative or positive thermal gradient as shown in Fig. 4 for the dry inlet flows. For the saturated and two-phase flows, the flow of liquid water in the channel has a tendency to distribute the heat more evenly down the flow channel. For the saturated inlet flows, a higher liquid phase velocity exists at 353 K than at 298 K resulting in a more uniform temperature distribution for the 353 K inlet case as shown in Fig. 4.

Since the liquid phase has an important effect on the mass, momentum, and thermal distributions of the gas phase, it might be desirable to indicate where and how much liquid water exists in the flow channels. Figure 6 shows the volume percent of liquid water in the flow channel for a dry inlet gas entering at different temperatures. The onset of liquid water production occurs over a range of 40 to 50% down the channel length for a dry inlet gas temperature ranging from 25 to 80 °C, respectively. The accumulation of this product water over many cells in the fuel cell stack would eventually cause lower reactant concentrations, as shown in Fig. 3, unless the gas stream is internally dehumidified. The production rate of water, Eq. (6), is dependent upon the fraction of water entering the cathode as governed by the parameter $f_c$. Note that this parameter value may assume a value larger than one since it is possible for water in the anode to migrate by electroosmotic effects and combine with the electrochemically produced water on the cathode side. The effects of this parameter on the fluid temperature, Fig. 7, shows that increases in the water production rate causes a decrease in the fluid temperature in the channel. This phenomena may be self-correcting in that the lower temperature in the channel may cause a lower temperature in the electrode through conduction and, hence, lower the electrochemical reaction rate. The complex relationship of the mass, momentum, and thermal distributions in the flow field is strongly dependent on the heat transfer effects. From a design viewpoint, enhanced fuel cell performance can be gained by considering these transport effects in designing fuel cell stacks. These design considerations can help minimize areas of electrochemical inactivity by preventing low reactant concentrations and by controlling undesirable thermal gradients that may lower reaction rates in the electrodes as well as influence the water management.

## SUMMARY

A mathematical model of the multi-component, two-phase flow in a fuel cell gas channel was developed and used to determine the mass, momentum, and thermal distributions in the flow field. It was shown that the oxygen concentration could obtain exceedingly low values when liquid water was introduced in the flow field as a result of changing the gas phase momentum. Thermal and liquid water distributions were shown indicating the complex water and thermal management issues associated with this system. The ability to predict the thermal and water behavior of the flow field can be applied to an entire fuel cell stack in order to obtain and understand better this phenomena which can aid in designing higher performing fuel cell stacks.

## REFERENCES


1) N.E. Vanderborgh, J. Hedstrom, and J.R. Huff, "Thermal Management of Advanced Fuel Cell Power Systems," P. 149, 25th IECEC, Reno, NV, August (1990).

2) J.D. Anderson, *Modern Compressible Flow*, McGraw-Hill, New York, (1990).

3) M.N. Ozisik, *Heat Transfer: A Basic Approach*, McGraw-Hill, New York (1985).

4) N.E. Vanderborgh, J.R. Huff, and J. Hedstrom, "Heat and Mass Transfer Effects in PEM Fuel Cells," P. 1637, 24th IECEC, Washington, D.C. (1989).


**Table 1: Base case parameter values for the single channel flow field model.**

| Parameter | Value |
|---|---|
| Channel length, $L$ | 160.0 cm |
| Channel width, $W$ | 0.127 cm |
| Channel depth, $D$ | 0.127 cm |
| Pressure, $P$ | 3.0 atm |
| Inlet temperature, $T$ | 298.15 K |
| Temperature in fuel cell, $T_{rxn}$ | 363.15 K |
| Temperature of wall @ inlet, $T_{wall}^{in}$ | 353.15 K |
| Temperature of wall @ outlet, $T_{wall}^{out}$ | 353.15 K |
| Inlet gas stoichiometry | 2 |
| Inlet liquid flow | 0 lpm |
| Current density, $j$ | 1.0764 A/cm$^2$ |
| Water fraction, $f_c$ | 1.0 |

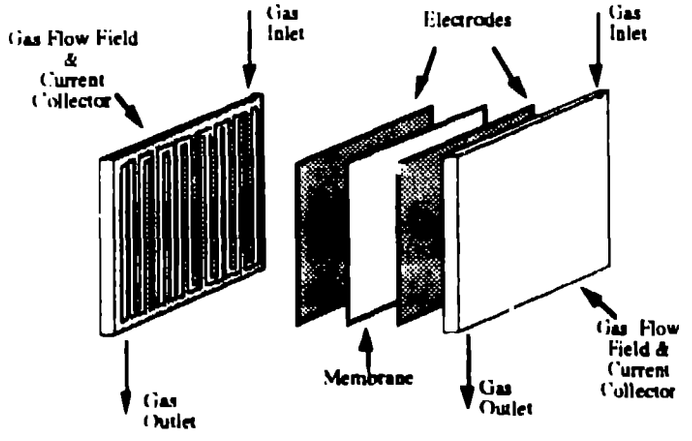


Figure 1. Schematic of a PEM fuel cell with a single channel gas flow field.

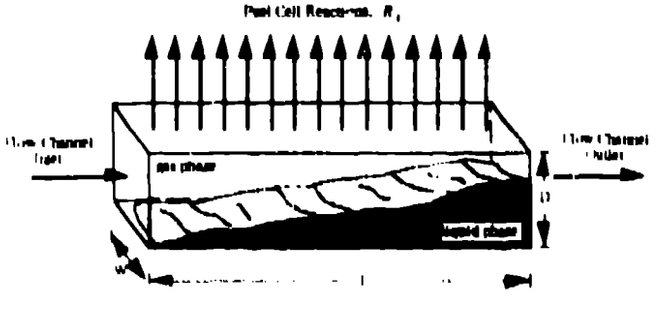

Figure 2. Two-phase representation of the gas channel in a PEM fuel cell flow field

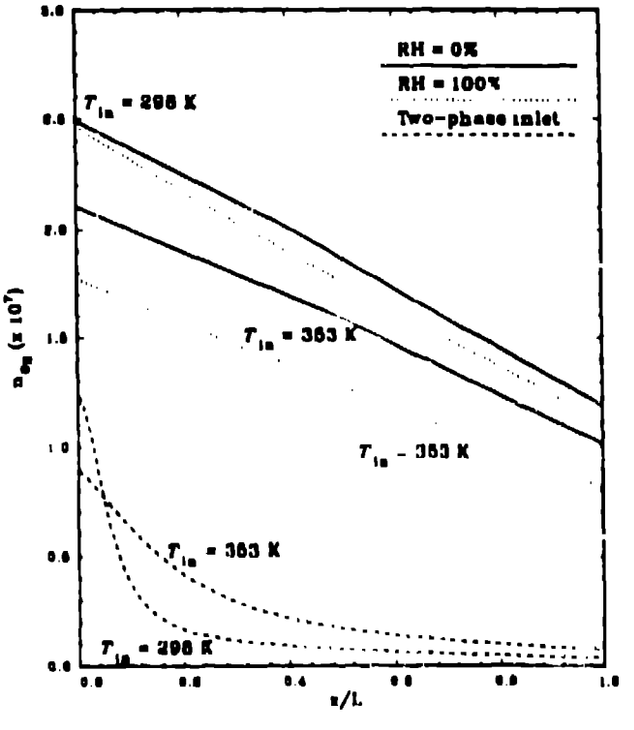


**Figure 3. Number of oxygen moles in the flow channel for different inlet relative humidities (RH) and inlet temperatures.**

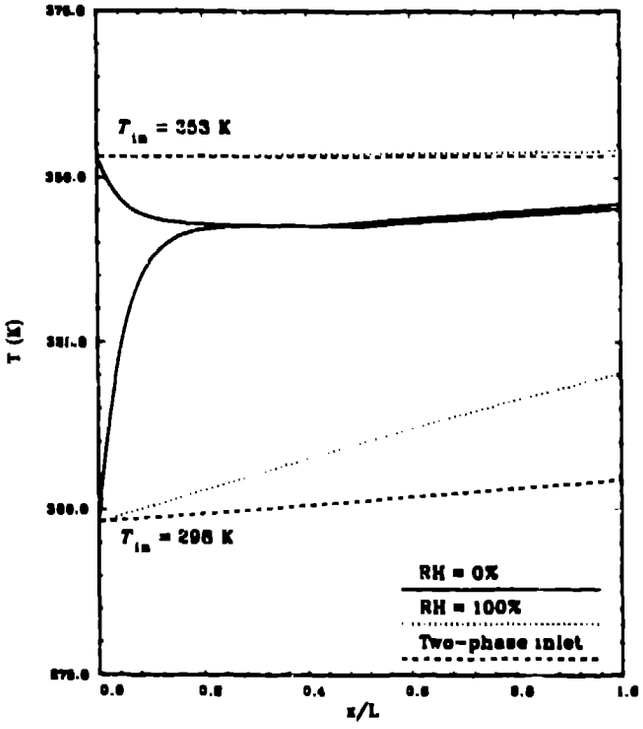


Figure 4. Temperature distribution in the flow channel for different inlet relative humidities (RH) and inlet temperatures.

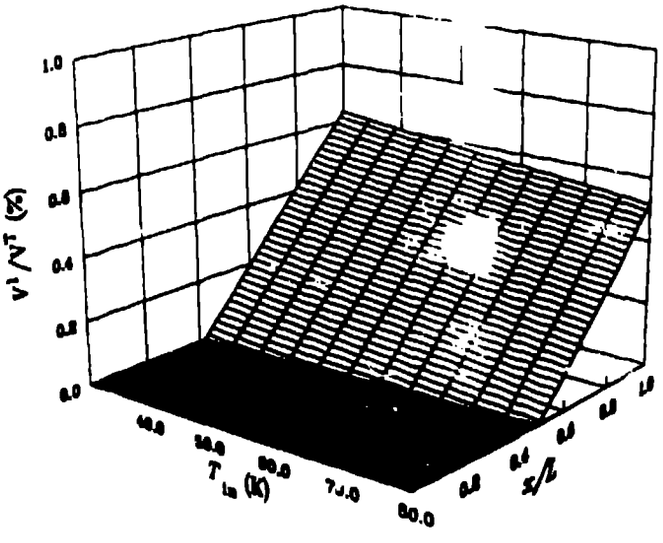


Figure 6. Volume percent of the liquid phase in the gas channel for a dry inlet gas at various inlet temperatures.

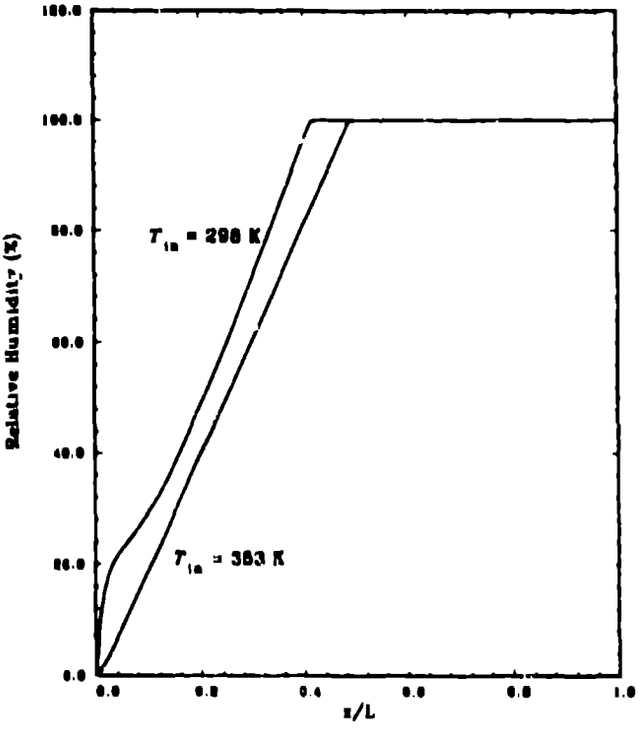


Figure 5. Variation of the relative humidity in the flow channel for a dry inlet gas.

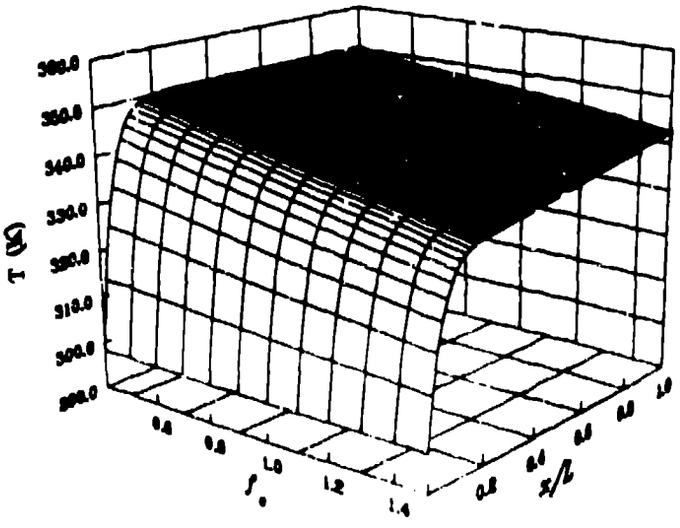


Figure 7. Fluid temperature distribution in the channel for a dry inlet gas entering at 298 K for different fractions ($f_o$) of the total water production rate.